



The effect of calcining temperatures on the phase purity and electric properties of $\text{CaCu}_3\text{Ti}_4\text{O}_{12}$ ceramics

Tao Li, Renzhong Xue, Junhong Hao, Yuncai Xue, Zhenping Chen*

Department of Technology and Physics, Zhengzhou University of Light Industry, Zhengzhou, 450002, People's Republic of China

ARTICLE INFO

Article history:

Received 31 July 2010

Received in revised form

20 September 2010

Accepted 26 September 2010

Available online 20 October 2010

Keywords:

Second phase

Permittivity

Non-ohmic property

Schottky barriers

ABSTRACT

$\text{CaCu}_3\text{Ti}_4\text{O}_{12}$ (CCTO) ceramics are prepared by the traditional solid-state reaction method under the same sintering conditions. The effect of calcining temperatures for the powders before sintering on the microstructure and electric properties of CCTO ceramics has been investigated. The XRD patterns for the powder calcined at 950°C show that some measure of second phases (CaTiO_3 , TiO_2 and CuO) can be found except a considerable amount of CCTO phase in them and the content of second phases decrease markedly as the calcining temperature is raised to 1000°C . The XRD patterns for the powder calcined at 1050°C indicate that the powder has been basically formed into a single CCTO phase except a small quantity of CaTiO_3 phase, which is attributed to CuO volatilizing in the calcining process. Furthermore, the XRD patterns for the CCTO pellets sintered at $1080^\circ\text{C}/10\text{ h}$ manifest that all the second phases have disappeared after the sintering process except that a very weak peak of CaTiO_3 can still be seen in the XRD pattern for the pellets made of the powder calcined at 1050°C . The electric properties measurement demonstrates that the lower calcining temperature for the raw powder is helpful to increase the values of permittivity and the higher calcining temperature is helpful to improve the non-ohmic properties. The non-ohmic characteristic has a behavior reverse to that of the permittivity, which can be ascribed to the change in the height of Schottky barriers.

© 2010 Elsevier B.V. All rights reserved.

1. Introduction

Recently, an unusual body-centered cubic perovskite material $\text{CaCu}_3\text{Ti}_4\text{O}_{12}$ (CCTO) has attracted much attention of researchers in scientific fields due to its exceptional dielectric properties, such as high dielectric permittivity ($\sim 10^4$ – 10^5) and low loss (less than 0.05) at low frequencies at room temperature and its good stability over a wide temperature range from 100 to 600 K [1–3]. Furthermore, structural studies have showed that CCTO has not any phase transitions down to 35 K [1,4]. Such material is very promising for capacitor applications and certainly for microelectronics, microwave devices (cell mobile phones for example), especially for the potential application in miniaturized electronic components/devices. Despite the fact that much research work has been done, including the experiment and theory, to reveal nature and origin of the giant dielectric constant of CCTO ceramics, it still remains controversial and unsolved to date. At present, a plausible explanation, an internal grain boundary barrier layer capacitance (IBLC) model at the grain boundaries between semiconducting grains [5,6], is accepted widely by the researchers. In addition to the intriguing dielectric property, CCTO has also presented excellent

non-ohmic behavior. Chung et al. have reported that CCTO exhibits nonlinear current–voltage characteristics even in the absence of any dopants and found that the nonlinear coefficient α of CCTO ceramics reaches the value of 912 when measured in the range of 5–100 mA [7]. Later, Marques et al. and Sun et al. have pointed out successively the nonlinear current–voltage characteristics of CCTO ceramics [8,9]. In similar studies, we have reported the nonlinear current–voltage characteristics of CCTO ceramics doped by Eu_2O_3 and sintered under different conditions [10,11]. The findings show that the grain boundary potential barrier (Schottky potential barriers) intrinsically existing in the grain boundary region between the conducting and n typical grains of perovskite ceramics [7] appear to play an important role in the non-ohmic behavior of CCTO ceramics; and it can act as an obstacle to hinder the current from flowing through the conductive bulk grains in polycrystalline specimens. In this paper, the raw material powders mixed with a certain stoichiometric ratio were calcined at different temperatures, and then sintered under the same conditions to synthesize CCTO ceramics. The effect of calcining temperatures on the microstructure and electric properties of the samples has been discussed.

2. Experimental procedure

Analytical grade powders of CaCO_3 , CuO and TiO_2 were weighed out in stoichiometric proportions, ball-milled in alcohol for 12 h, dried and then calcined at 950°C , 1000°C and 1050°C for 10 h, respectively. The calcined powders were remilled for

* Corresponding author. Tel.: +86 371 63556807; fax: +86 37163556150.
E-mail address: chaodaotai@126.com (Z. Chen).

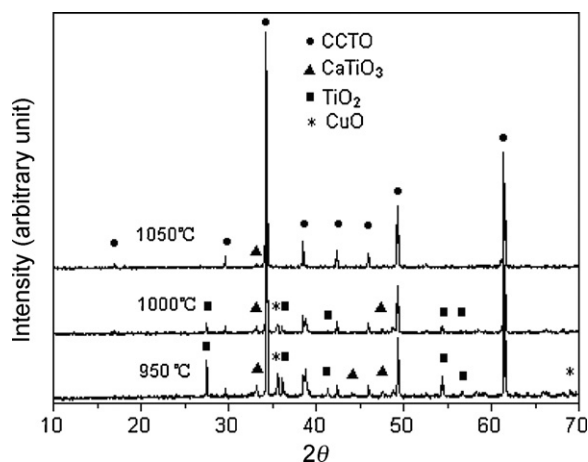


Fig. 1. XRD powder patterns for the calcined CCTO powders.

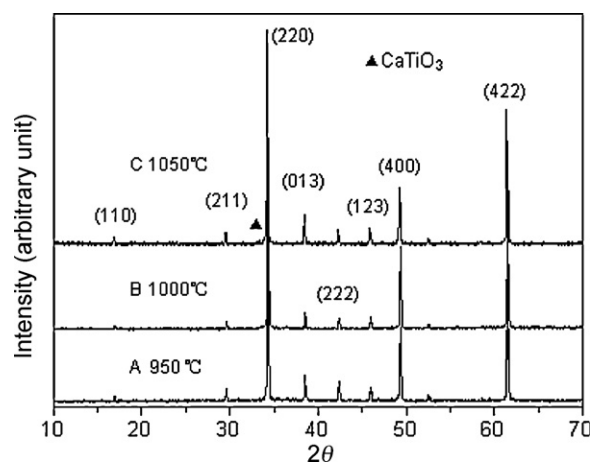


Fig. 2. XRD powder patterns for the sintered CCTO ceramics.

2 h and granulated by adding PVA, then pressed into pellets (150 MPa) with a diameter of 12.0 mm and thickness of 2.0 mm. Finally the pellets were sintered in air at 1080 °C for 10 h and they were named samples A, B and C corresponding to the powders calcined at 950 °C, 1000 °C and 1050 °C. X-ray diffraction (XRD) with Cu K α radiation ($\lambda = 0.1541$ nm) was performed to examine the phase constitution of the calcined powders and the sintered specimens at room temperature. A high-voltage measuring unit (Trek model 609B) was used to measure the current–voltage (I – V or J – E) characteristics while the pellets were put into silicon oil. The dielectric properties and impedance spectrum of the pellets were determined using an Agilent 4294A Precision Impedance Analyzer from 40 Hz to 110 MHz. The nonlinear coefficient α values were calculated in terms of the formula:

$$\alpha = \frac{\lg(I_2/I_1)}{\lg(V_2/V_1)}$$

where α is calculated when $I_1 = 1$ mA, $I_2 = 10$ mA, respectively. V_1 and V_2 are, respectively, the voltage at current I_1 and I_2 . The breakdown electric field (threshold electric field) (E_b) is obtained when a current density of 1 mA flows through the pellets.

3. Results and discussions

Densities of the sintered pellets were measured by the Archimedes method. The relative density for A, B, and C is 94.9%, 92.3%, 90.3%, respectively (the theoretical density of CCTO is 4.9 g/cm³ [12]).

The XRD patterns for the powders calcined at different temperatures are shown in Fig. 1. Compared with the major peaks of the pseudo-cubic CCTO provided by the Powder Diffraction File database (PDF 75-2188), the diffraction peaks for the powder calcined at 950 °C show that a considerable amount of CCTO phase has been formed, but some measure of second phases (CaTiO₃, TiO₂ and CuO) are contained. Compared with the powder calcined at 1000 °C, the content of second phases for the powder calcined at 1000 °C decreases drastically. As the calcining temperature rises to 1050 °C, the powder has been basically formed into a single CCTO phase except traces of CaTiO₃ phase, which indicates that the volatilization of CuO occurs in the calcining process. Fig. 2 presents the XRD patterns for the CCTO pellets sintered at 1080 °C/10 h. It is interesting that all the second phases have disappeared after the sintering process for samples A and B, and all the major diffraction peaks are matched with those of the standard PDF database [JCPDF File No. 75-2188]. However, a very weak peak of CaTiO₃ can still be seen in the XRD pattern of sample C, which confirms the analysis above. In addition, CuO can be decomposed into Cu₂O and O₂ when the temperature is higher than 1026 °C (the decomposition temperature of CuO). But Cu₂O phase cannot be observed in the XRD patterns of the powders especially in that of the powder calcined at 1050 °C, which suggests that only traces of CuO can be decomposed.

The frequency dependence of permittivity (ϵ_r) and dielectric loss ($\tan\delta$) at room temperature of the samples are given in Fig. 3(a) and

(b). It can be found that all the samples show giant permittivity of $\epsilon_r > 6000$ below 1 MHz and the permittivity versus frequencies plots basically shows a plateau in a broad frequency range followed by a strong drop for about 10⁷ Hz as previously reported [3,9] except that ϵ_r of sample A decreases slowly with the increase of frequency below 10 kHz. The ϵ_r decreases with the increase of calcining temperature, accordingly ϵ_r of the sample A is largest, about 2 times that of sample B and more than 2.3 times that of sample B below 1 MHz. The $\tan\delta$ of all the samples is obviously frequency dependent and

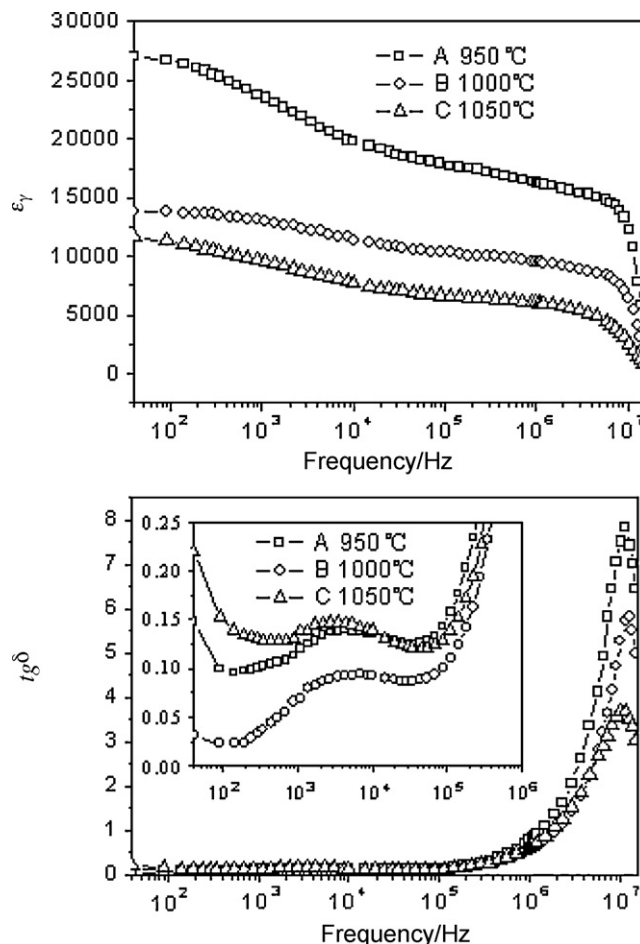


Fig. 3. Frequency dependence of dielectric properties of CCTO ceramics calcined at different temperatures.

Table 1
Frequency dependence of ϵ_r and $\tan \delta$ of CCTO ceramics calcined at different temperatures.

Samples	100 Hz		1 kHz		10 kHz		100 kHz		1 MHz	
	ϵ_r	$\tan \delta$	ϵ_r	$\tan \delta$	ϵ_r	$\tan \delta$	ϵ_r	$\tan \delta$	ϵ_r	$\tan \delta$
950 °C	26,500	0.098	23,600	0.11	19,800	0.13	17,300	0.15	16,300	0.76
1000 °C	13,800	0.023	13,100	0.066	11,400	0.092	10,300	0.1	9600	0.52
1050 °C	11,200	0.14	9600	0.13	7800	0.14	6600	0.13	6000	0.61

begins to increase quickly above 10^6 Hz. The change trend of $\tan \delta$ versus frequency indicates that the dielectric properties of all the samples undergo a very weak relaxation related to grain boundary between 1 kHz and 10 kHz and a Debye relaxation related to grains near 1 GHz. However, the $\tan \delta$ of sample B has the smallest value compared with that of sample A and C. The $\tan \delta$ of sample A, B and C at 1 kHz is 0.12, 0.069 and 0.14, respectively. In order to clearly find the dielectric property, the values of ϵ_r and $\tan \delta$ of the samples at selected frequencies are listed in Table 1.

The behaviors of dielectric properties of the samples are closely related to the calcining temperatures, because more second phases CuO and TiO₂ after calcining process can be formed into low melting point eutectic [13], which is conducive to the growth of grain and improvement in the densification of the samples in the sintering process. Combined with the densities measurement of the samples, it can be confirmed that sample A has larger grain size and thinner grain boundary layer than sample B and Sample B has larger grain size and thinner grain boundary layer than sample C. The permittivity (ϵ_r) is highly dependent upon the grain size and the thickness of the grain boundary layer [14], and the larger grain size and thinner grain boundary layer can lead to larger permittivity of CCTO. In addition, the deviation from stoichiometry because of the volatilization of CuO in the calcining process is also the cause to decrease permittivity ϵ_r for sample C.

Fig. 4 exhibits the current density (J) versus electric field (E) plots obtained for the samples. It can be found that a strong non-linear relationship between J and E is exhibited for all the samples. The breakdown electric field of samples A, B and C is 0.43 kV/cm, 0.68 kV/cm and 1.12 kV/cm corresponding to the voltage of 85.7 V, 135.8 V and 224.5 V, respectively. According to the formula in the above, the coefficient α values calculated at room temperature are 7.5, 9.8 and 12.5 in the current range of 1–10 mA corresponding to the samples A, B and C, respectively. It clearly indicates that E_b and α values of the samples are also closely related to calcining temperatures and they have a behavior reverse to the permittivity, which is in accordance with the results we have reported [11]. The behaviors between dielectric and non-ohmic properties related to

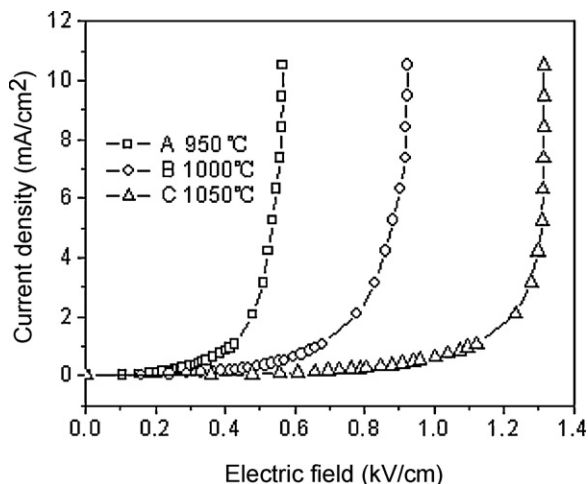


Fig. 4. Nonlinear J - E behaviors of CCTO ceramics calcined at different temperatures.

calcining temperatures suggest that a suitable calcining temperature can be selected to obtain the CCTO ceramics with desired electric properties in the manufacturing of electronic components.

In polycrystalline CCTO ceramics, double (back-to-back) Schottky potential barriers are created at interfaces between n-type grains due to charge trapping at acceptor states, resulting in bending of the conduction band across the grain boundary. This band bending produces an effective potential barrier of height [15]. The effect of Schottky barriers at grain boundaries on the I - V behavior can be described in terms of the following equation [9]:

$$\ln \left(\frac{J}{AT^2} \right) = \left(\frac{\beta}{k_B T} \right) E^{1/2} - \frac{\Phi_B}{k_B T} \quad (2)$$

where A is Richardson's constant ($=1200 \text{ mA mm}^{-2} \text{ k}^{-2}$), Φ_B is the height of Schottky barriers k_B is the Boltzman constant, β is a constant related to the potential barrier width, T is the temperature (K). According to the Eq. (2), the relation between the $\ln(J/AT^2)$ and $E^{1/2}$ for the samples at room temperature has been obtained in Fig. 5 which presents a good linear relationship of $\ln(J/AT^2)$ and $E^{1/2}$ below the breakdown electric field (E_b), but that the plots become deviated from the linear relationship as the electric field is higher than E_b .

The obtained values of Φ_B from the intercepts of the lines in Fig. 5 for samples A, B and C are 0.82 eV, 0.84 eV and 0.89 eV, respectively which are close to the reported barrier height of 0.79–0.90 eV [16]. It can be considered that the lower calcining temperature for the powders leads to the higher Φ_B in the sintering process, which results in the increase of the nonlinear coefficient α and the breakdown electric field.

In the absence of a dc bias, the relation between the permittivity ϵ_r and the height of Schottky barriers Φ_B can be described in terms of the following formula:

$$\Phi_b = \frac{eN_s^2}{8\epsilon_0\epsilon_r N_d} \quad (3)$$

where e is the electronic charge, N_s is the acceptor (surface charge) concentration, $\epsilon_0 = 8.854 \times 10^{-14} \text{ F/cm}$, ϵ_r is the relative permittivity of the material and N_d is the charge carrier concentration in the grains.

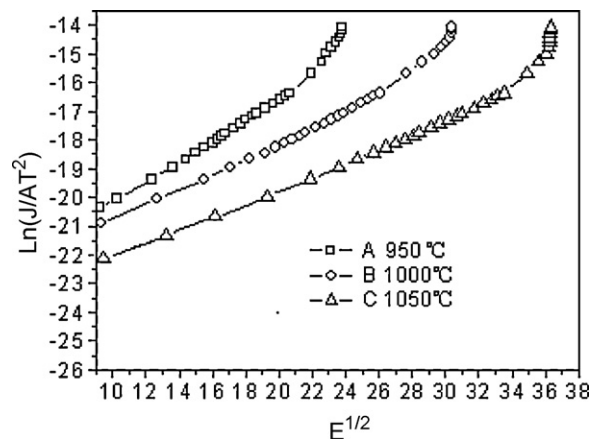


Fig. 5. Relation between the $\ln(J/AT^2)$ and $E^{1/2}$ for the samples at room temperature.

It can be found that the permittivity ϵ_r is inversely proportional to the height of Schottky barriers Φ_B . Therefore, the reverse behaviors between the permittivity and the non-ohmic characteristic can be ascribed to the change in the height of Schottky barriers Φ_B .

4. Conclusions

- (1) The strong effect of calcining temperatures for the powders before sintering process on the microstructure of CCTO ceramics can be found. Some measure of second phases (CaTiO_3 , TiO_2 and CuO) can be observed in the XRD patterns for the powder calcined at 950°C . The content of second phases decreases with the increase of calcining temperature. As the calcining temperature rises to 1050°C , the powder has been basically formed into a single CCTO phase except a small quantity of CaTiO_3 phase because of the volatilization of CuO in the calcining process.
- (2) The electric properties measurement shows that the lower calcining temperature for the raw powder is helpful to increase the values of permittivity and the higher calcining temperature is helpful to improve the non-ohmic properties. So, it is very important to select a suitable calcining temperature in preparing the CCTO ceramics with desired electric properties. The non-ohmic characteristic has a behavior reverse to that of the permittivity, which can be ascribed to the change in the height of Schottky barriers.

Acknowledgements

This study is supported by National Natural Science Foundation of China (Project No. 10875107), The Natural Science Foundation of

Henan (No. 082300440080), and The Basic Research Plan on Natural Science of the Education Department of Henan Province (Grant No. 2010B140016).

References

- [1] A.P. Ramirez, M.A. Subramanian, M. Gardel, G. Blumberg, D. Li, T. Vogt, S.M. Shapiro, *Solid State Commun.* 115 (2000) 217–220.
- [2] C.C. Homes, T. Vogt, S.M. Shapiro, S. Wakimoto, A.P. Ramirez, *Science* 293 (2001) 673–676.
- [3] V. Brizé, G. Gruener, J. Wolfman, K. Fatyeyeva, M. Tabellout, M. Gervais, F. Gervais, *Mater. Sci. Eng. B* 129 (2006) 135–138.
- [4] M.A. Subramanian, A.W. Sleight, *Solid State Sci.* 4 (2002) 347–351.
- [5] A.R. West, T.B. Adams, F.D. Morrison, D.C. Sinclair, *J. Eur. Ceram. Soc.* 24 (2004) 1439–1448.
- [6] R.K. Grubbs, E.L. Venturini, P.G. Clem, J.J. Richardson, B.A. Tuttle, G.A. Samara, *Phys. Rev. B* 72 (2005) 104111.
- [7] S.Y. Chung, I.D. Kim, S.J.L. Kang, *Nat. Mater.* 3 (2004) 774–778.
- [8] V.P.B. Marques, A. Ries, A.Z. Simoes, M.A. Ramirez, J.A. Varela, E. Longo, *Ceram. Int.* 33 (2007) 1187–1190.
- [9] Dun-Lu Sun, Ai-Ying Wu, Shao-Tang Yin, *J. Am. Ceram. Soc.* 91 (2008) 169–173.
- [10] Tao Li, Zhenping Chen, Fanggao Chang, Junhong Hao, Jincang Zhang, *J. Alloys Compd.* 484 (2009) 718–722.
- [11] Tao Li, Zhenping Chen, Yuling Su, Lei Su, Jincang Zhang, *J. Mater. Sci.* 44 (2009) 6149–6154.
- [12] M. Ranabrata, S. Anshuman, S. Amarnath, S.E. Himadri, *Ferroelectrics* 326 (2005) 103–108.
- [13] F.H. Lu, F.X. Fang, Y.S. Chen, *J. Eur. Ceram. Soc.* 21 (2001) 1093–1097.
- [14] B. Shri Prakash, K.B.R. Varma, *Physica B* 382 (2006) 312–319.
- [15] Timothy B. Adams, Derek C. Sinclair, Anthony R. West, *Phys. Rev. B* 73 (2006) 094124.
- [16] G.Z. Zang, J.L. Zhang, P. Zheng, J.F. Wang, C.L. Wang, *J. Phys. D: Appl. Phys.* 38 (2005) 1824–1827.